RSC Sustainability

ROYAL SOCIETY OF CHEMISTRY

PAPER

View Article Online
View Journal | View Issue

Cite this: *RSC Sustainability*, 2025, **3**, 4162

Nitro-functionalized imidazolium salts as acidic catalysts for cellulose degradation in ionic liquids

Flávia C. Sonaglio, Wellington D. G. Gonçalves, Virgínia S. Souza, Cecília A. Silveira and Jackson D. Scholten *

Received 15th October 2024
Accepted 4th August 2025

DOI: 10.1039/d4su00645c

rsc.li/rscsus

Nitro-functionalized imidazolium salts were applied as acidic catalysts for the degradation of cellulose into 5-hydroxymethylfurfural (HMF). The catalytic systems based on [NO_2HMIm][X] (X = TsO, Cl, NTf_2, CF_3CO_2), dissolved in [BMIm][Cl], were capable of producing HMF, glucose, fructose, formic acid, and levulinic acid as products of cellulose degradation at 130 °C. In particular, HMF was obtained in up to 17% yield using 10.8 mol% of [NO_2HMIm][TsO], representing one of the most active protic imidazolium salts reported in the literature for the transformation of cellulose under relatively mild conditions. Indeed, this work presents cost-effective and easily synthesized nitro-functionalized imidazolium salts as efficient catalysts for biomass conversion, offering a sustainable alternative to conventional SO_3H-based imidazolium ILs. Therefore, the strategy of modifying the acidity of a protic imidazolium salt by incorporating a nitro group in the imidazolium ring was successfully achieved, as observed in the degradation of cellulose, and can be extended to other acid-catalyzed reactions of biomass-derived compounds.

Sustainability spotlight

Currently, the demand for renewable energy sources to replace fossil fuels has significantly increased. In this context, the use of inexpensive and abundant raw materials for the synthesis of compounds with potential applications in energy systems has attracted the attention of many researches. Thus, the conversion of biomass-derived compounds (cellulose, carbohydrates, sugars) into higher value-added products is of great interest from the perspective of a sustainable system for industrial applications. In this work, efficient catalytic systems based on nitro-imidazolium acidic salts dissolved in an ionic liquid were developed for the degradation of cellulose into 5-hydroxymethylfurfural (HMF). The strategy of attaching a nitro group to the imidazolium cation resulted in an acidic salt capable of catalyzing the production of up to 17% yield of HMF from cellulose degradation at 130 °C. Therefore, this study presents a simple, robust, and sustainable catalytic system for cellulose degradation, which can be further extended to the conversion of other substrates through acid catalysis.

1 Introduction

Ionic liquids (ILs) are widely recognized as environmentally friendly solvents, particularly in catalysis.[1–5] Beyond their role as green solvents, ILs possess remarkable solvation abilities, enabling them to dissolve a broad spectrum of compounds.[6–10] Among their most intriguing applications is the dissolution of biopolymers such as lignin and cellulose,[11–17] making them valuable tools for biomass conversion into high-value chemicals. One of the key target products in this context is 5-hydroxymethylfurfural (HMF), a versatile compound with applications as a fuel, solvent, and precursor for various chemicals.[18–20]

Cellulose degradation to HMF typically relies on acid catalysts, including acidic ILs, which can function as both solvents and catalysts. However, a major challenge in using ILs as catalysts lies in their acidity profiles. While Brønsted acid ILs exhibit high Brønsted acidity, they generally possess moderate to low Lewis acidity, characterized by their electrophilicity. Consequently, traditional inorganic metal-based Lewis acids have often been used alongside ILs, with both species proposed to play a role in the rate-limiting steps of the degradation reaction, particularly in the isomerization of glucose to fructose, which is primarily governed by the Lewis acidity of the catalyst.[21,22] A more ideal system for the conversion of cellulose to HMF would eliminate the need for metals, thereby simplifying the process. In fact, the use of metal-free catalytic systems for cellulose degradation offers advantages such as lower cost, reduced environmental impact, and improved sustainability, making the process more attractive for producing high-value-added products. The use of sulfonated ILs as acidic catalysts for the degradation of biomass-derived compounds is extensively reported in the literature.[23,24] As an alternative to these traditional SO_3H-based imidazolium ILs, our group demonstrated the feasibility of attaching a nitro group to the imidazolium ring, yielding simple and cost-effective protic nitro-functionalized imidazolium salts with high Brønsted and Lewis acidities.[25] Generally, the advantages of using protic imidazolium salts may

Laboratory of Molecular Catalysis, Institute of Chemistry, UFRGS, Av. Bento Gonçalves, 9500, Agronomia, CEP 91501-970, Porto Alegre-RS, Brazil. E-mail: jackson.scholten@ufrgs.br

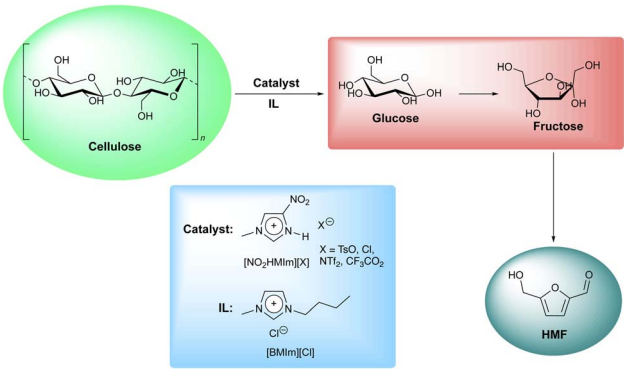

Scheme 1 Degradation of cellulose to HMF catalyzed by acidic nitro-functionalized imidazolium salts in an IL.

be attributed to their higher biodegradability in water compared to aprotic counterparts.[26] Moreover, protic ILs with shorter alkyl side chains, particularly those in which the alkyl group at the 1-position of the imidazolium ring is replaced with hydrogen,[27] tend to be less toxic than those with longer chains.[28] It was also observed that incorporating a methyl group into the imidazolium ring enhances its antimicrobial activity.[29] Therefore, the nitro-imidazolium salts developed by our group represent sustainable alternatives that align with current environmental demands. In addition, these compounds have previously demonstrated promising catalytic activity in the acetylation of glycerol to triacetin,[25] suggesting their potential for broader applications in acid-catalyzed reactions, such as cellulose degradation.

In this study, we evaluated [NO_2HMIm][X] (X = TsO, Cl, NTf_2, CF_3CO_2) salts as acidic catalysts for cellulose degradation in [BMIm][Cl] (Scheme 1), a widely used and efficient solvent for cellulose dissolution.[15,23,24] Our preliminary results showed that using 10.8 mol% of [NO_2HMIm][TsO] at 130 °C yielded up to 17% HMF, demonstrating the potential of these nitro-functionalized imidazolium salts as effective catalysts for biomass valorization.

2 Experimental

2.1 Materials and methods

Microcrystalline cellulose powder (particle size approximately 20 μm) and 5-hydroxymethyl-2-furaldehyde (98% purity), used as a standard for producing the GC-FID calibration curve, were purchased from Sigma-Aldrich/Merck and used as received without purification. Acetone (UV/HPLC grade) and methanol (99.8%) were purchased from Vetec and used as received without purification. Nitric acid (70%), hydrochloric acid (37%), trifluoroacetic acid (99%), and sulfuric acid (98%) were used as received.

^{1}H and ^{13}C NMR spectra were acquired using a Bruker Ascend 400 (400 MHz and 101 MHz, respectively). ^{1}H NMR spectra were acquired with 32 scans and a relaxation delay of 1 s for compound characterization and for the control experiment without cellulose, whereas a longer relaxation delay of 30 s was employed for the analysis of mixtures from cellulose degradation reactions. ^{13}C NMR spectra were recorded using 512 scans and a relaxation delay of 2 s for the characterization of imidazolium salts, while 12 400 scans with the same relaxation delay were used for analyzing the reaction mixtures. FTIR spectra were acquired using a Bruker Alpha Fourier-T spectrometer with a Platinum ATR module, applying 50 scans at a resolution of 4 cm^{-1}. Gas chromatography with a flame ionization detector (GC-FID) was performed using an Agilent 7890A system coupled with an Agilent Autosampler 7693 and a DB-WAX column (30 m, 0.25 mm, 0.25 μm). UV-vis analysis was performed with a Shimadzu UV-vis 2450 spectrophotometer. TGA of the imidazolium salts was performed in a SDT Q600 TA Instruments equipment using nitrogen gas with a flow rate of 100 mL min^{-1}, heating rate of 10 °C min^{-1}, and a maximum temperature of 700 °C.

2.2 Synthesis of the compounds

2.2.1 1-Butyl-3-methylimidazolium chloride. [BMIm][Cl] was synthesized using a similar route reported in the literature.[30] The FTIR, ^{1}H NMR, and ^{13}C NMR spectra are shown in Fig. S1, S7, and S8, respectively.

^{1}H NMR (400 MHz, DMSO-d_6) δ = 9.52 (t, J = 1.7 Hz, 1H), 7.88 (t, J = 1.8 Hz, 1H), 7.80 (t, J = 1.7 Hz, 1H), 4.20 (t, J = 7.1 Hz, 2H), 3.87 (s, 3H), 1.81–1.70 (m, 2H), 1.23 (m, 2H), 0.88 (t, J = 7.4 Hz, 3H). ^{13}C NMR (101 MHz, DMSO-d_6) δ = 136.7, 123.6, 122.3, 48.4, 35.7, 31.4, 18.8, 13.3.

2.2.2 1-Methyl-3-*H*-4-nitroimidazolium tosylate. The nitro-functionalized imidazolium salt [NO_2HMIm][TsO] was synthesized according to our previously described procedure in the literature.[25] The synthetic route begins with the preparation of 4(5)-nitroimidazole (Section 2.2.3), followed by the synthesis of 1-methyl-4-nitroimidazole (Section 2.2.4). Finally, 1-methyl-3-*H*-4-nitroimidazolium tosylate was obtained, with experimental details provided in Section 2.2.5.

2.2.3 Synthesis of 4(5)-nitroimidazole. Initially, 4(5)-nitroimidazole was prepared by adding nitric acid (0.93 mol) to imidazole (0.15 mol) under an ice bath with magnetic stirring. Subsequently, sulfuric acid (0.41 mol) was added, and the reaction mixture was kept under reflux overnight (approximately 15 h). After completion, the system was cooled in a freezer, and the white precipitate was filtered, washed with distilled water, and dried under vacuum at 60 °C.

2.2.4 Synthesis of 1-methyl-4-nitroimidazole. 4(5)-Nitroimidazole (88.4 mmol) and K_2CO_3 (0.13 mol) were dispersed in acetonitrile (150 mL). A solution of iodomethane (6.6 mL in 50 mL of acetonitrile, 106 mmol) was added dropwise to the mixture while stirring under an ice bath. The solution was stirred at 65 °C overnight (approximately 15 h) and then filtered. The product was extracted from the solid phase by using a dichloromethane and methanol mixture (95 : 5 v/v). The solvents were removed under vacuum, and the remaining solid was recrystallized using 2-propanol.

2.2.5 Synthesis of 1-methyl-3-*H*-4-nitroimidazolium tosylate. 1-Methyl-4-nitroimidazole (7.9 mmol) dispersed in acetonitrile (4 mL) was added to an equimolar amount of *p*-toluenesulfonic acid monohydrate in acetonitrile (7 mL) under an

ice bath and stirred for 30 minutes. The solution was heated to 60 °C and stirred overnight (approximately 15 h). Afterward, the solvent was removed under vacuum at 60 °C. The salt was washed four times with diethyl ether and dried under vacuum at 60 °C, yielding a white solid (yield: 88%, melting point: 119.6–120.4 °C).

^{1}H NMR (400 MHz, DMSO-d_6) δ = 8.36 (d, J = 1.4 Hz, 1H), 7.80 (d, J = 1.5 Hz, 1H), 7.49 (d, J = 8.1 Hz, 2H), 7.13 (d, J = 7.9 Hz, 2H), 3.74 (s, 3H), 2.29 (s, 3H). ^{13}C NMR (101 MHz, DMSO-d_6) δ = 146.9, 144.8, 138.5, 138.2, 128.4, 125.6, 122.7, 34.3, 20.9.

2.2.6 1-Methyl-3-*H*-4-nitroimidazolium chloride. The [NO_2HMIm][Cl] salt was synthesized following our published procedure.[25] 1-Methyl-4-nitroimidazole (27.4 mmol) dispersed in acetonitrile (18 mL) was added to an equimolar amount of hydrochloric acid (2.3 mL of aqueous solution). The solution was stirred for 30 minutes under an ice bath, and then heated to 60 °C for 24 h. Afterward, the solvent was removed under vacuum at 60 °C using a rotary evaporator. The salt was washed five times with diethyl ether and dried under vacuum at 60 °C. Finally, the solid was recrystallized from ethanol to afford a white solid (yield: 76%, melting point: 135.5–136.1 °C).

^{1}H NMR (400 MHz, DMSO-d_6) δ = 8.35 (d, J = 1.4 Hz, 1H), 7.80 (d, J = 1.5 Hz, 1H), 3.75 (s, 3H). ^{13}C NMR (101 MHz, DMSO-d_6) δ = 146.9, 138.1, 122.6, 34.2.

2.2.7 1-Methyl-3-*H*-4-nitroimidazolium bis(trifluoromethanesulfonyl)imide. 1-Methyl-3-*H*-4-nitroimidazolium chloride (3.0 mmol) dispersed in water (4 mL) was added to an equimolar amount of lithium bis(trifluoromethanesulfonyl)imide in water (2 mL). The solution was stirred for 1.5 h. Afterward, the product was extracted with dichloromethane (30 mL). Then, the organic solvent was dried over $MgSO_4$, filtered, and evaporated under vacuum using a rotary evaporator. The salt was recrystallized from ethanol to afford a white solid (yield: 42%, melting point: 108.0–108.8 °C).

^{1}H NMR (400 MHz, DMSO-d_6) δ = 8.35 (d, J = 1.4 Hz, 1H), 7.80 (d, J = 1.4 Hz, 1H), 3.75 (s, 3H). ^{13}C NMR (101 MHz, DMSO-d_6) δ = 146.9, 138.0, 122.5, 121.1, 117.9, 34.2.

2.2.8 1-Methyl-3-*H*-4-nitroimidazolium trifluoroacetate. 1-Methyl-4-nitroimidazole (7.9 mmol) dispersed in acetonitrile (6 mL) was added to an equimolar amount of trifluoroacetic acid (0.61 mL). The solution was stirred for 30 minutes under an ice bath, and then heated to 60 °C for 24 h. Afterward, the solvent was removed under vacuum at 60 °C using a rotary evaporator, yielding a white solid (yield: 55%, melting point: 136.2–137.5 °C).

^{1}H NMR (400 MHz, DMSO-d_6) δ = 8.35 (d, J = 1.4 Hz, 1H), 7.80 (d, J = 1.5 Hz, 1H), 3.75 (s, 3H). ^{13}C NMR (101 MHz, DMSO-d_6) δ = 146.9, 138.0, 122.5, 34.2.

2.3 Cellulose degradation reaction

The method used for cellulose degradation was based on the procedure described in the literature.[31] Cellulose (0.1 g, 0.62 mmol, calculated based on the molar mass of the anhydroglucose unit, $C_6H_{10}O_5$) and [BMIm][Cl] (2.0 g, 11.45 mmol) were magnetically stirred in a two-necked round-bottom glass flask (10 mL) equipped with a closed water-cooled reflux condenser over an oil bath at 100 °C until complete dissolution of the cellulose. Subsequently, deionized water (0.2 g, 11.1 mmol) and varying amounts of the acid catalyst (0.033, 0.066 or 0.167 mmol) were added to the flask, which was then quickly heated to 130 °C, initiating reflux. Reaction time zero was defined as the moment when the reaction mixture reached 130 °C. Small samples were collected at different reaction times for characterization analyses (FTIR, ^{1}H/^{13}C NMR, and GC-FID). These samples were placed in small sealed vials, immediately cooled with cold water, weighed, and stored in a refrigerator (5–10 °C) for analysis.

2.4 Quantification of HMF

The quantification of HMF was performed using GC-FID and ^{1}H NMR analyses, with both techniques providing consistent and reproducible results.

2.4.1 GC-FID analysis. To separate the [BMIm][Cl] from the reaction mixture samples, an amount of acetone (approximately 25 times the mass of the sample) was mixed with the sample in a test tube. The mixture was then heated to its boiling point, and a few drops of methanol were added to fully dissolve [BMIm][Cl] (about 4 drops of methanol for every 1 mL of acetone used). The solutions were stored in the refrigerator overnight (approximately 15 h) to allow [BMIm][Cl] crystals to precipitate. The test tubes were then placed in a centrifuge to separate the [BMIm][Cl] crystals and any other solids (presumably undissolved cellulose and humins) from the supernatant containing HMF. An aliquot of 1 mL was taken from the supernatant and diluted with 1 mL of acetone. The solution was analyzed by GC-FID to determine the concentration of HMF. Each sample was injected three times using automatic injection. Eqn (1) was used to calculate the yield of HMF:

$$\text{HMF yield } \% = \frac{\text{final } m \text{ of HMF}/M \text{ of HMF}}{\text{initial } m \text{ of cellulose}/M \text{ of anhydroglucose unit}} \times 100 \quad (1)$$

where m is the mass and M is the molar mass. The molar mass (M) of cellulose $(C_6H_{10}O_5)_n$ was calculated based on the molar mass of the anhydroglucose unit (162.14 g mol^{-1}). A calibration curve was constructed using data from the injection of standard solutions of HMF (1–5 μL) at different concentrations (2×10^{-5}, 8×10^{-5}, 4×10^{-4} mol L^{-1}), which were appropriate for the scale of product observed in the reaction.

2.4.2 ^{1}H NMR analysis. After the reaction was completed, the system was cooled in an ice bath, and a 20–30 mg sample of the solution was collected. The sample was dissolved in 400 μL of DMSO-d_6 in a glass vial and then transferred to the NMR tube. The signals of the imidazolium ring from [BMIm][Cl] were used as an internal standard to quantify the amount of HMF formed, as described by eqn (1). For comparison, standard HMF was also analyzed in DMSO-d_6: ^{1}H NMR (DMSO-d_6) δ = 9.54 (s, 1H), 7.48 (d, J = 3.5 Hz, 1H), 6.60 (d, J = 3.5 Hz, 1H), 5.56 (t, J = 5.9 Hz, 1H), 4.51 (d, J = 5.7 Hz, 2H). ^{13}C NMR (101 MHz, DMSO-d_6) δ = 178.0, 162.2, 151.8, 124.5, 109.7, 56.0.

Note: Similarly to HMF, levulinic acid and formic acid were quantified from the NMR spectra using eqn (1).

2.5 Brønsted acidity of the imidazolium salts

2.5.1 Hammett acidity function (H_0). The Hammett acidity function (H_0)[32] values of the nitro-functionalized imidazolium salts were determined using UV-vis spectroscopy, following a previously reported procedure.[33] In these measurements, 8×10^{-6} mol L^{-1} of 4-nitroaniline (Hammett indicator) was added to a solution of the imidazolium salts (5×10^{-5} mol L^{-1}) dissolved in water or DMSO. The H_0 values were calculated using eqn (2):

$$H_0 = pK_a(IH^+)_{aq} + \log\left(\frac{[I]}{[IH^+]}\right) \quad (2)$$

where $pK_a(IH^+)_{aq}$ represents the pK_a of the protonated indicator in an aqueous solution (0.99), while [I] and [IH^+] denote the molar concentrations of the unprotonated (with a maximum absorbance at 380 nm in water and 389 nm in DMSO) and protonated forms of the indicator in the protic salt solutions, respectively.

2.5.2 FTIR. The FTIR study was conducted by adapting a previously reported procedure in the literature.[23] For the analysis, 2–5 mg of the nitro-functionalized imidazolium salt was mixed with 30 μL of pyridine, and the resulting solution was analyzed using FTIR. In the present study, the band at 1543 cm^{-1}, referring to the pyridinium cation, was used as a standard for comparison.

3 Results and discussion

Initially, all nitro-functionalized imidazolium salts were characterized using FTIR, ^{1}H NMR, and TGA. FTIR analysis confirmed the presence of characteristic bands for the compounds (Fig. S2–S5). In addition, ^{1}H/^{13}C NMR analyses validated their chemical structures (Fig. S9–S16). TGA analysis demonstrated that the imidazolium salts remained thermally stable up to 150 °C (Fig. S19–S22). The protic imidazolium salt [NO_2HMIm][TsO] was chosen as a model acidic catalyst for the degradation of cellulose in [BMIm][Cl] at 130 °C. The reaction using 10.8 mol% catalyst was investigated with FTIR by analyzing the final reaction mixture at different time intervals (Fig. 1). The degradation of cellulose is observed through the reduction of the broad bands around 3400 cm^{-1}, indicating the breakdown of O–H groups in cellulose. Additionally, a decrease in the bands between 1100 and 1020 cm^{-1} is noted, as this region is characteristic of C–O stretching in cellulose. Moreover, the appearance of a peak around 1667 cm^{-1} suggests the presence of molecules containing C=O groups, one of which is HMF. In the standard compound, HMF exhibits a C=O stretching peak at 1656 cm^{-1} (Fig. S6). Furthermore, a small peak is observed at 1521 cm^{-1} due to the C=C bond, while another peak around 1021 cm^{-1} is likely associated with C–O stretching. In the HMF standard, these peaks appear at 1519 cm^{-1} and 1016 cm^{-1}, respectively (Fig. S6).

These preliminary results persuaded us to further investigate the catalytic system based on nitro-functionalized imidazolium salts under different conditions and to quantify HMF production. Other compounds, such as glucose, fructose, formic acid, levulinic acid, and humins (undesirable dark-colored solids commonly generated in this type of reaction), are also likely present. In this study, we decided to evaluate the formation of HMF in more detail due to its high potential for use in renewable energy applications. Notably, a control reaction using only the [BMIm][Cl]/water mixture yielded up to 2% HMF and formic acid, along with trace amounts of levulinic acid (0.1%) at 130 °C. Additionally, signals typically attributed to glucose and fructose were identified by ^{13}C NMR, although accurate quantification by ^{1}H NMR proved difficult (Fig. S23 and S24). Another control experiment for cellulose degradation, conducted in the absence of water, resulted in HMF and formic acid yields of up to 6% and 5%, respectively, along with trace amounts of levulinic acid (0.2%) when [NO_2HMIm][TsO] (10.8 mol%) was used as the catalyst (Fig. S25). In this control reaction, only HMF was identified by ^{13}C NMR analysis (Fig. S26). The transformation of cellulose into HMF was primarily catalyzed by the acidic nitro-imidazolium salt [NO_2HMIm][TsO], dissolved in a [BMIm][Cl]/water mixture at 130 °C, under varying catalyst loadings and reaction times (Fig. 2). It was observed that at 5.4 mol% catalyst, the HMF yield was almost negligible, while the addition of 10.8 mol% catalyst produced HMF with a yield of up to 17%.

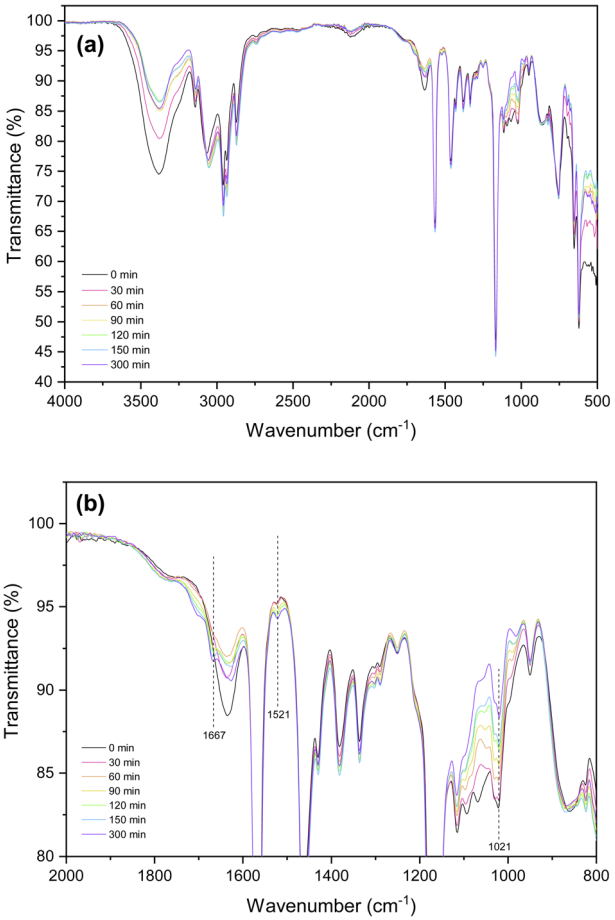

Fig. 1 (a) Infrared spectra of the cellulose degradation reaction catalyzed by [NO_2HMIm][TsO] (10.8 mol%). (b) Zoomed-in region showing the signals of products: C=O stretching at 1667 cm^{-1}, C=C stretching at 1521 cm^{-1} and C–O stretching at 1021 cm^{-1}.

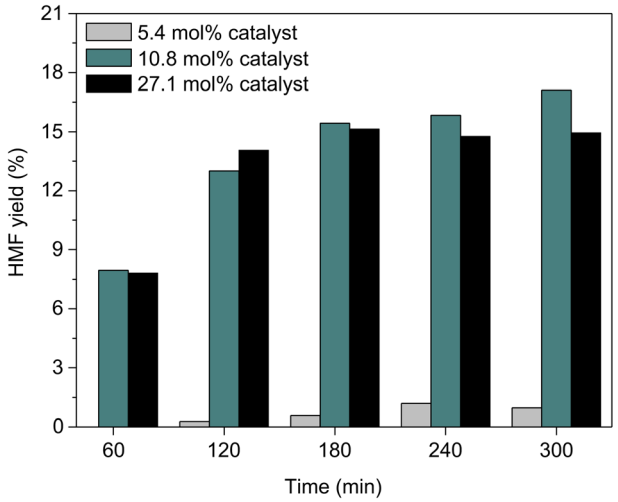

Fig. 2 HMF yield obtained from the degradation of cellulose using [NO_2HMIm][TsO] in [BMIm][Cl] at 130 °C with varying reaction times and catalyst amounts. Yields were determined by GC. The average error in the reactions was estimated to be 2% based on triplicate experiments.

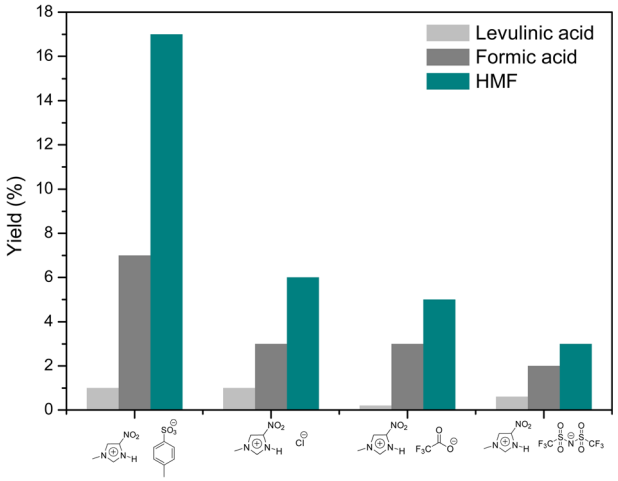

Fig. 3 HMF, levulinic acid, and formic acid yields from cellulose degradation using different protic nitro-functionalized imidazolium salts [NO_2HMIm][X] (X = TsO, Cl, NTf_2, CF_3CO_2) in [BMIm][Cl]. Reaction conditions: cellulose (0.1 g), [BMIm][Cl] (2 g), deionized water (0.2 g), 10.8 mol% catalyst, 130 °C, and 5 h. Yields were determined by ^{1}H NMR. The average error in the reactions was estimated to be 2% based on triplicate experiments.

Moreover, the yield appeared to slightly decrease at concentrations as high as 27.1 mol%, likely due to the conversion of HMF into other compounds, such as levulinic acid, and the formation of humins. For reactions using 5.4 and 27.1 mol% of catalyst, the color gradient is possibly due to the increase in the concentration of products (Fig. S27). To clarify this aspect, an experiment was conducted in the absence of cellulose under the same reaction conditions (nitro-imidazolium salt dissolved in a [BMIm][Cl]/water mixture at 130 °C). After the reaction, the mixture remained colorless, and ^{1}H NMR analysis confirmed that neither the [BMIm][Cl] nor the nitro-imidazolium salt had decomposed (Fig. S28). Consequently, the color gradient is likely due to product formation, which appears to stabilize around 300 minutes, suggesting that extending the reaction time beyond this point may not improve the HMF yield in this system. Therefore, 10.8 mol% catalyst appears to be the optimal amount for the present system. Notably, these results indicate that the synergistic effect of water as an additive and the acidic catalyst is crucial for enhancing product formation. In addition, this result makes it one of the most active protic imidazolium salts reported in the literature for the transformation of cellulose under relatively mild conditions. ^{1}H NMR analysis of the reaction solution confirmed the presence of HMF, as evidenced by signals at 9.54, 7.50, 6.60, and 4.48 ppm (Fig. S29), which correspond to those observed in the spectrum of standard HMF (Fig. S17). Additionally, ^{1}H NMR analysis revealed a signal at 8.18 ppm corresponding to formic acid, and a signal at 2.07 ppm likely attributed to the methyl group of levulinic acid. Further confirmation of HMF formation was provided by ^{13}C NMR, which displayed characteristic signals at 178.0, 162.9, 150.4, 109.7, and 55.8 ppm (Fig. S30). Peaks observed in the region of 61.0–105.2 ppm may be attributed to glucose, fructose, and cellulose.

Based on the optimized reaction conditions established using the acidic salt [NO_2HMIm][TsO] in [BMIm][Cl] (10.8 mol% catalyst, 300 min reaction time), other protic nitro-functionalized imidazolium salts were evaluated as acidic catalysts for cellulose degradation (Fig. 3). Under optimized conditions, cellulose degradation using [NO_2HMIm][Cl], [NO_2-HMIm][NTf_2], and [NO_2HMIm][CF_3CO_2] as catalysts yielded 6%, 3%, and 5% HMF, respectively (Fig. 3 and S31, S33, S35). In these cases, levulinic acid and formic acid were also detected and quantified by ^{1}H NMR analysis, with signals at 2.07 ppm for levulinic acid and 8.18–8.20 ppm for formic acid (Fig. S31, S33, and S35). The ^{1}H NMR spectra also exhibited peaks likely corresponding to cellulose between 4.50 and 5.50 ppm, and to glucose/fructose in the region of 3.00–5.50 ppm. Quantification of these products by ^{1}H NMR was not possible due to signal overlap in the corresponding spectral region. Therefore, these compounds were not included as products in Fig. 3. For the reaction using [NO_2HMIm][Cl], the presence of HMF was confirmed by ^{13}C NMR analysis, with characteristic peaks at 178.0, 150.4, 109.6, and 55.7 ppm (Fig. S32). In the catalytic systems employing [NO_2HMIm][NTf_2] (Fig. S34) and [NO_2-HMIm][CF_3CO_2] (Fig. S36), signals at 109.7 ppm and 55.8 ppm were also attributed to HMF. Notably, in the ^{13}C NMR spectra, signals likely corresponding to glucose, fructose, and cellulose were observed in the region of 60.9–105.2 ppm; however, in some cases, these signals appeared with low intensity in the spectra.

To support the explanation of the observed catalytic activities, the Brønsted acidity of the nitro-functionalized imidazolium salts was determined. The acidity was evaluated using two complementary methods: (i) UV-vis analysis in the presence of *p*-nitroaniline to determine Hammett function (H_0) values (Fig. 4a, Table 1) and (ii) FTIR analysis with pyridine, monitoring the band at 1543 cm^{-1}, which corresponds to the pyridinium cation (Fig. 4b). According to the acidity scale based on

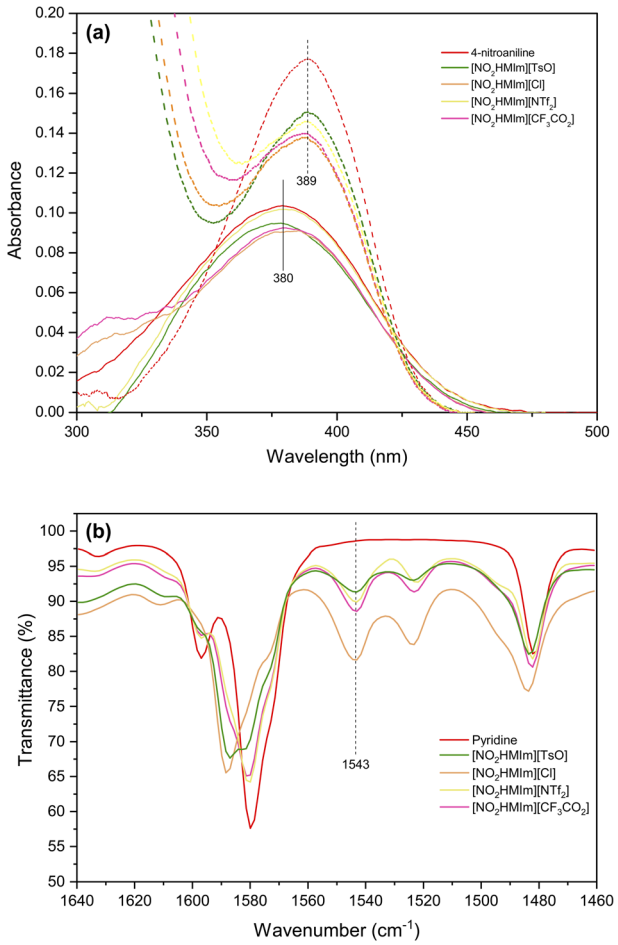

Fig. 4 Brønsted acidity of the nitro-functionalized imidazolium salts: (a) UV-vis analysis in the presence of *p*-nitroaniline (solid line: water as solvent, band at 380 nm; dashed line: DMSO as solvent, band at 389 nm) for the determination of Hammett function (H_0) values; (b) FTIR analysis with pyridine, monitoring the band at 1543 cm^{-1} corresponding to the pyridinium cation.

H_0 values, the following order was observed in aqueous solution: [NO_2HMIm][Cl] > [NO_2HMIm][CF_3CO_2] > [NO_2HMIm][TsO] > [NO_2HMIm][NTf_2]. The H_0 values were also measured in DMSO, where the acidity followed the order: [NO_2HMIm][Cl] > [NO_2HMIm][CF_3CO_2] > [NO_2HMIm][NTf_2] > [NO_2HMIm][TsO]. The different acidity position of the imidazolium salt [NO_2HMIm][TsO] is likely due to competitive protonation between water and *p*-nitroaniline in aqueous solution. This is supported by the ^{1}H NMR spectrum of the salt in DMSO-d_6 (Fig. S9), where the signal of residual water is shifted, likely as a result of protonation by the nitro-imidazolium tosylate. Additionally, the Brønsted acidity of the imidazolium salts was evaluated using FTIR analysis in the presence of pyridine. The qualitative acidity order was determined as [NO_2HMIm][Cl] > [NO_2HMIm][CF_3CO_2] > [NO_2HMIm][NTf_2] > [NO_2HMIm][TsO], aligning with the acidity order obtained from the Hammett function. The results suggest that the nature of the anion plays a significant role in determining the acidic properties of the catalyst. Surprisingly, the small amounts of products observed in reactions employing the most acidic salts ([NO_2HMIm][Cl] and [NO_2HMIm][CF_3CO_2]) contrast with the expected results based on the relative acidities of the imidazolium salts. Thus, it is likely that acidity is not the only factor influencing this reaction; other effects, such as the stabilization of intermediates, may play a fundamental role in this system. In fact, the less acidic salt [NO_2HMIm][TsO] generated a higher yield of HMF compared to the other salts. Moreover, the higher yield of HMF relative to formic and levulinic acids suggests that the reaction stops at HMF rather than proceeding to its further degradation (Fig. 3). This result may be attributed to the enhanced stabilization of intermediates by the [NO_2HMIm][TsO] salt through hydrogen bonding and π-stacking interactions with both the imidazolium cation and the tosylate anion, favoring the formation of HMF.

It is important to note that this sustainable catalytic system produces HMF yields comparable to those of acidic catalysts based on SO_3H-functionalized ILs reported in the literature (Table 2 and Fig. 5). In fact, depending on the reaction conditions and the IL structure, the present catalytic system based on NO_2-functionalized imidazolium salt exhibits HMF yield that is comparable to, or even higher than, that of the SO_3H-functionalized ILs containing the HSO_4^- anion (entries 2 and 3, Table 2). Moreover, the use of SO_3H-functionalized ILs has achieved HMF yields of up to 28%; however, these results were obtained under harsher reaction conditions (entry 3, Table 2). Notably, the present catalytic system operates under a relatively mild temperature (130 °C), and the catalyst loading used in this study (10.8 mol%) is substantially lower than those commonly reported for similar SO_3H-functionalized IL-based systems, demonstrating the high intrinsic activity and efficiency of the Brønsted acid salt [NO_2HMIm][TsO]. Since nitro-functionalized imidazolium salts represent a new class of acidic catalysts, there

Table 1 Hammett acidity function (H_0) parameters of the [NO_2HMIm][X] salts[a]

Entry	Catalyst	A_{max}	[I] (%)	[IH^+] (%)	H_0
1	4-Nitroaniline	0.104 (0.177)	100 (100)	0 (0)	— (—)
2	[NO_2HMIm][TsO]	0.095 (0.158)	91 (89)	9 (11)	2.01 (1.91)
3	[NO_2HMIm][Cl]	0.091 (0.138)	88 (78)	12 (22)	1.83 (1.54)
4	[NO_2HMIm][NTf_2]	0.103 (0.146)	99 (82)	1 (18)	3.00 (1.66)
5	[NO_2HMIm][CF_3CO_2]	0.093 (0.140)	89 (79)	11 (21)	1.92 (1.57)

[a] The values in parentheses refer to the experiments conducted in DMSO.

Table 2 Comparison of selected acidic ionic liquid systems for cellulose hydrolysis with the present catalytic system

Entry	Solvent	Catalyst (mol%)	T (°C)	t (min)	Additive (g)	HMF yield (%)	Ref.
1	[BMIm][Cl]	**1** (10.8)	130	300	H_2O (0.2)	17	This work
2	[BMIm][Cl]/DMF	**2** (159)[a]	100	60	H_2O (0.08)	15	23
		3 (128)[a]				10	
3	4-Methyl-2-pentanone	**3** (154)	150	300	H_2O (1)	16	34
		4 (125)				22	
		5 (132)				23	
		6 (120)				25	
		7 (161)				17	
		8 (132)				28	
		9 (125)				25	
		10 (270)				15	

[a] The catalyst mol% was estimated assuming an IL density of 1 g mL^{-1}.

are many possibilities for modifying their chemical and physical properties to develop a more efficient catalytic system. This class of compounds could also feasibly replace metal-based additives, which are often used in conjunction with Brønsted acid ILs to enhance catalytic activity.

The present work represents a significant advancement in acid-catalyzed biomass conversion by utilizing nitro-functionalized imidazolium salts as catalysts. The proposed nitro-functionalized salts offer a more sustainable alternative to conventional Brønsted acid SO_3H-based imidazolium ILs. By strategically enhancing the acidity of the imidazolium cation through the incorporation of a nitro group with electron-withdrawing properties, this approach eliminates the need for multiple SO_3H functional groups and associated counterions. The ease of handling and broad applicability of these novel salts further underscore their potential as sustainable and economically viable alternatives for biomass-derived transformations, reinforcing their importance in green chemistry and renewable energy applications. This study aligns with Goal 7 of the United Nations Sustainable Development Goals (SDGs), which promotes affordable, reliable, and sustainable energy. By developing an efficient catalytic system using nitro-functionalized imidazolium salts as acid catalysts for cellulose degradation into HMF, this work advances sustainable energy solutions by enhancing the valorization of biomass-derived feedstocks. These innovations reduce reliance on fossil resources and support the development of renewable energy and bio-based chemicals, reinforcing sustainability and clean energy production.

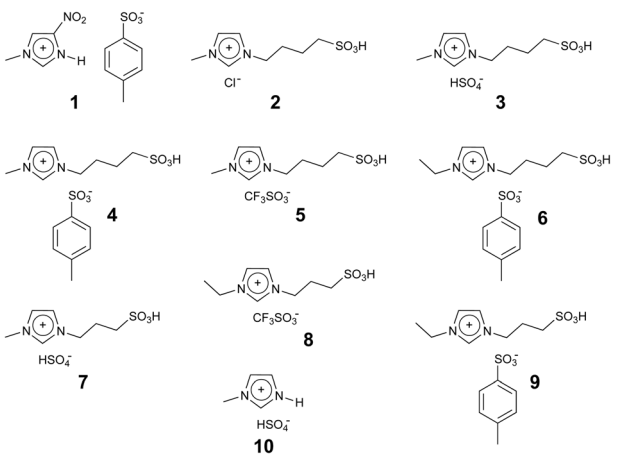

Fig. 5 Examples of acidic ILs reported in the literature as catalysts for cellulose degradation, along with the acidic IL used in this study.

3.1 Cost analysis

The total cost analysis of raw materials, including both the catalyst synthesis and the cellulose hydrolysis reaction, for obtaining 1 g of HMF is shown in Table S1. First, it is important to note that a direct comparison between the final value in Table S1 and the commercial price is not ideal. Commercial prices include costs related to labor, equipment, packaging, company profit, and other factors, whereas the proposed HMF cost in this study is based solely on raw material expenses. However, even a superficial comparison can provide an initial idea of the economic feasibility of large-scale industrial production. The commercial price of HMF (>99%, Sigma-Aldrich/Merck) was listed as US$ 64.20 per gram. In this study, the cost was calculated based on a reaction using 10.8 mol% of [NO_2HMIm][TsO], which produced HMF with a 17% yield (0.0132 g HMF). The total cost of this reaction system for HMF production was determined to be US$37.03 per gram (Table S1). Notably, improvements in reaction conditions and the process could increase the yield and reduce production costs. Considering that HMF is typically marketed on a small to medium scale, and that the cost estimate in this study is based on small-scale laboratory production from biomass, the potential for industrial-scale production appears promising. However, it is important to note that the cost analysis provided here is a preliminary estimate focused solely on raw material expenses and does not account for purification or downstream processing steps. Although the isolation of HMF was not performed in this study, its feasibility was considered; however, the complexity of the ionic liquid–water reaction medium, the presence of humins, and the need to optimize solvent-extraction and purification protocols present technical and

economic challenges that warrant further investigation in future work.

4 Conclusions

In summary, this study presents nitro-functionalized imidazolium salts as effective and sustainable acidic catalysts for the degradation of cellulose in ionic liquids. Our results show that [NO_2HMIm][TsO] dissolved in [BMIm][Cl] can produce HMF with a yield of up to 17% using 10.8 mol% catalyst at 130 °C. Notably, other products such as glucose, fructose, formic acid, and levulinic acid were also observed in these catalytic systems. Therefore, the strategy of modifying the acidity of a protic imidazolium salt by incorporating a nitro group into the imidazolium ring resulted in a competent acid catalyst capable of transforming cellulose into HMF. In particular, this nitro-functionalized imidazolium salt dissolved in an IL can be considered a simple, cost-effective, and sustainable alternative compared to other IL-based acidic catalysts reported in the literature. These findings are significant for the development of more active metal-free catalytic systems for degrading biomass-derived compounds into higher-value products.

Author contributions

F. C. Sonaglio: data curation, formal analysis, investigation, methodology; W. D. G. Gonçalves: data curation, formal analysis, investigation, methodology; V. S. Souza: formal analysis, investigation; C. A. Silveira: data curation, formal analysis, investigation; J. D. Scholten: conceptualization, funding acquisition, resources, supervision, writing – original draft, writing – review & editing.

Conflicts of interest

There are no conflicts to declare.

Data availability

The data supporting this article have been included as part of the SI.

Supplementary information is available. See DOI: **https://doi.org/10.1039/d4su00645c**.

Acknowledgements

The authors thank the following Brazilian agencies for their financial support: CAPES (finance code 001) and CNPq (309111/2021-8).

Notes and references

1 J. Dupont, B. C. Leal, P. Lozano, A. L. Monteiro, P. Migowski and J. D. Scholten, *Chem. Rev.*, 2024, **124**, 5227–5420.
2 P. Wasserscheid and W. Keim, *Angew. Chem., Int. Ed.*, 2000, **39**, 3773–3789.
3 J. Dupont, R. F. de Souza and P. A. Z. Suarez, *Chem. Rev.*, 2002, **102**, 3667–3691.
4 J. P. Hallett and T. Welton, *Chem. Rev.*, 2011, **111**, 3508–3576.
5 J. D. Scholten, B. C. Leal and J. Dupont, *ACS Catal.*, 2012, **2**, 184–200.
6 Q. Liu, M. H. A. Janssen, F. van Rantwijk and R. A. Sheldon, *Green Chem.*, 2005, **7**, 39–42.
7 X. Li, A. Van den Bossche, T. Vander Hoogerstraete and K. Binnemans, *Chem. Commun.*, 2018, **54**, 475–478.
8 Y. Zheng, X. Xuan, J. Wang and M. Fan, *J. Phys. Chem. A*, 2010, **114**, 3926–3931.
9 S. Doblinger, D. S. Silvester and M. Costa Gomes, *Fluid Phase Equilib.*, 2021, **549**, 113211.
10 M. C. Corvo, J. Sardinha, S. C. Menezes, S. Einloft, M. Seferin, J. Dupont, T. Casimiro and E. J. Cabrita, *Angew. Chem., Int. Ed.*, 2013, **52**, 13024–13027.
11 A. Brandt, J. Gräsvik, J. P. Hallett and T. Welton, *Green Chem.*, 2013, **15**, 550–583.
12 A. Farrán, C. Cai, M. Sandoval, Y. Xu, J. Liu, M. J. Hernáiz and R. J. Linhardt, *Chem. Rev.*, 2015, **115**, 6811–6853.
13 H. Wang, G. Gurau and R. D. Rogers, *Chem. Soc. Rev.*, 2012, **41**, 1519–1537.
14 T. J. Szalaty, Ł. Klapiszewski and T. Jesionowski, *J. Mol. Liq.*, 2020, **301**, 112417.
15 R. P. Swatloski, S. K. Spear, J. D. Holbrey and R. D. Rogers, *J. Am. Chem. Soc.*, 2002, **124**, 4974–4975.
16 T. Heinze, K. Schwikal and S. Barthel, *Macromol. Biosci.*, 2005, **5**, 520–525.
17 H. Zhang, J. Wu, J. Zhang and J. He, *Macromol.*, 2005, **38**, 8272–8277.
18 Y. He, L. Deng, Y. Lee, K. Li and J.-M. Lee, *ChemSusChem*, 2022, **15**, e202200232.
19 T. Su, D. Zhao, Y. Wang, H. Lü, R. S. Varma and C. Len, *ChemSusChem*, 2021, **14**, 266–280.
20 F. A. Kucherov, L. V. Romashov, K. I. Galkin and V. P. Ananikov, *ACS Sustain. Chem. Eng.*, 2018, **6**, 8064–8092.
21 F. Tao, H. Song, J. Yang and L. Chou, *Carbohydr. Polym.*, 2011, **85**, 363–368.
22 F. Tao, H. Song and L. Chou, *ChemSusChem*, 2010, **3**, 1298–1303.
23 F. Jiang, Q. Zhu, D. Ma, X. Liu and X. Han, *J. Mol. Catal. A: Chem.*, 2011, **334**, 8–12.
24 L. Hu, G. Zhao, X. Tang, Z. Wu, J. Xu, L. Lin and S. Liu, *Bioresour. Technol.*, 2013, **148**, 501–507.
25 E. M. Morais, I. B. Grillo, H. K. Stassen, M. Seferin and J. D. Scholten, *New J. Chem.*, 2018, **42**, 10774–10783.
26 B. Peric, J. Sierra, E. Martí, R. Cruañas, M. A. Garau, J. Arning, U. Bottin-Weber and S. Stolte, *J. Hazard. Mater.*, 2013, **261**, 99–105.
27 C. Pretti, C. Chiappe, I. Baldetti, S. Brunini, G. Monni and L. Intorre, *Ecotoxicol. Environ. Saf.*, 2009, **72**, 1170–1176.
28 M. Amde, J. F. Liu and L. Pang, *Environ. Sci. Technol.*, 2015, **49**, 12611–12627.
29 D. Demberelnyamba, K.-S. Kim, S. Choi, S.-Y. Park, H. Lee, C.-J. Kim and I.-D. Yoo, *Bioorg. Med. Chem.*, 2004, **12**, 853–857.

30 J. Dupont, C. S. Consorti, P. A. Z. Suarez and R. F. de Souza, *Org. Synth.*, 2002, **79**, 236.
31 H. Cai, C. Li, A. Wang, G. Xu and T. Zhang, *Appl. Catal. B Environ.*, 2012, **123–124**, 333–338.
32 L. P. Hammett and A. J. Deyrup, *J. Am. Chem. Soc.*, 1932, **54**, 2721–2739.
33 J. Wei, L. Yu, L. Yan, W. Bai, X. Lu and Z. Gao, *RSC Adv.*, 2021, **11**, 32559–32564.
34 F. Tao, H. Song and L. Chou, *Bioresour. Technol.*, 2011, **102**, 9000–9006.